JOURNAL OF VIROLOGY, Apr. 2005, p. 5163–5173 Vol. 79, No. 8
0022-538X/05/$08.00+0 doi:10.1128/JVI.79.8.5163–5173.2005

A Proline-Rich Region in the Coxsackievirus 3A Protein Is Required for the Protein To Inhibit Endoplasmic Reticulum-to-Golgi Transport

Els Wessels,[1] Daniël Duijsings,[1] Richard A. Notebaart,[2] Willem J. G. Melchers,[1] and Frank J. M. van Kuppeveld[1]*

Department of Medical Microbiology, Nijmegen Center for Molecular Life Sciences, University Medical Center Nijmegen,[1] and Center for Molecular and Biomolecular Informatics, University of Nijmegen,[2] Nijmegen, The Netherlands

Received 13 July 2004/Accepted 17 November 2004

The ability of the 3A protein of coxsackievirus B (CVB) to inhibit protein secretion was investigated for this study. Here we show that the ectopic expression of CVB 3A blocked the transport of both the glycoprotein of vesicular stomatitis virus, a membrane-bound secretory marker, and the alpha-1 protease inhibitor, a luminal secretory protein, at a step between the endoplasmic reticulum (ER) and the Golgi complex. CVB 3A contains a conserved proline-rich region in its N terminus. The importance of this proline-rich region was investigated by introducing Pro-to-Ala substitutions. The mutation of Pro^{19} completely abolished the ability of 3A to inhibit ER-to-Golgi transport. The mutation of Pro^{14}, Pro^{17}, or Pro^{20} also impaired this ability, but to a lesser extent. The mutation of Pro^{18} had no effect. We also investigated the possible importance of this proline-rich region for the function of 3A in viral RNA replication. To this end, we introduced the Pro-to-Ala mutations into an infectious cDNA clone of CVB3. The transfection of cells with in vitro-transcribed RNAs of these clones gave rise to mutant viruses that replicated with wild-type characteristics. We concluded that the proline-rich region in CVB 3A is required for its ability to inhibit ER-to-Golgi transport, but not for its function in viral RNA replication. The functional relevance of the proline-rich region is discussed in light of the proposed structural model of 3A.

Enteroviruses (poliovirus, coxsackievirus, echovirus, and several unnamed viruses) are small viruses that contain a 7.5-kb single-stranded RNA genome with positive polarity. The genomic RNA harbors one large open reading frame that encodes the viral polyprotein. This polyprotein is proteolytically processed by virally encoded proteases into the individual capsid proteins and the nonstructural replication proteins ($2A^{pro}$, 2B, 2C, 3A, 3B, $3C^{pro}$, and $3D^{pol}$) as well as the relatively stable precursor proteins 2BC, 3AB, and $3CD^{pro}$ (22, 33). Replication of the viral RNA (vRNA) takes place in replication complexes in conjunction with secretory pathway-derived membrane vesicles that accumulate in the cytoplasm of the infected cell (2, 24). Enteroviruses are nonenveloped, cytolytic viruses that do not rely on an intact secretory pathway to release their virus progeny. Instead, poliovirus (PV) has been shown to induce a general blockage of protein secretion (8). Through the individual expression of the different nonstructural proteins of PV, Doedens and Kirkegaard have shown that proteins 2B and 3A are each sufficient to inhibit transport through the secretory pathway (8). The step blocked by the 2B protein is presently unknown. The expression of the PV 3A protein resulted in the accumulation in the ER of both the G protein of vesicular stomatitis virus (VSVG) and the alpha-1 protease inhibitor (A1PI) (7, 8). Moreover, the inhibition of ER-to-Golgi transport by PV 3A was shown to result in a reduced secretion of cytokines and interleukins (6), a down-regulation of major histocompatibility complex class I (MHC I)-dependent antigen presentation (3), and resistance to tumor necrosis factor alpha (TNF-α)-induced apoptosis (by elimination of the TNF receptor from the cell surface) (19). These findings represent unique examples of the evasion of both innate and acquired immune responses as well as the extrinsic apoptotic pathway by viral interference with secretory pathway trafficking. The mechanism by which the 3A protein inhibits secretory transport is as yet unknown.

In addition to its function in manipulating intracellular protein transport, the enterovirus 3A protein is involved in multiple steps in the process of vRNA replication. The 3A protein is a small hydrophobic protein (87 to 89 amino acids [aa]) that contains a C-terminal hydrophobic anchor which is responsible for its membrane association (29). Several studies have shown that mutations in 3A give rise to defects in vRNA synthesis (1, 10, 12, 35). The membrane-bound precursor 3AB is most likely the donor of VPg (i.e., 3B), the peptide that serves as the primer for vRNA synthesis, to the membranous replication complex (21). Moreover, 3AB serves as a cofactor for the binding of 3CD to the 5′ and 3′ termini of the RNA genome (11), the polymerase activity of $3D^{pol}$ (16, 20), and the autocatalytic processing of $3CD^{pro}$ to $3C^{pro}$ and $3D^{pol}$ (18).

For this study, we investigated whether the function of the enterovirus 3A proteins in interfering with endoplasmic reticulum (ER)-to-Golgi transport is conserved in the closely related coxsackievirus B (CVB). Expression of the CVB3 3A protein was indeed sufficient to inhibit ER-to-Golgi transport.

* Corresponding author. Mailing address: Department of Medical Microbiology, Nijmegen Center for Molecular Life Sciences, University Medical Center Nijmegen, P.O. Box 9101, 6500 HB Nijmegen, The Netherlands. Phone: (31) 24 3617574. Fax: (31) 24 3540216. E-mail: f.vankuppeveld@ncmls.ru.nl.

All enterovirus 3A proteins contain a proline-rich region in their N termini. The biological significance of this proline-rich region, which may be involved in protein-protein interactions, was investigated by the individual expression of CVB3 3A mutants and the introduction of these mutations into an infectious cDNA clone of CVB3. Our results indicate that the integrity of this proline-rich region is required for the inhibition of ER-to-Golgi transport by the CVB3 3A protein, but not for its functions in vRNA replication.

MATERIALS AND METHODS

Cells and viruses. Buffalo green monkey (BGM) kidney cells were grown in minimal essential medium (MEM) (Gibco) supplemented with 10% fetal bovine serum. COS-1 cells were grown in Dulbecco's modified Eagle's medium (Gibco) supplemented with 10% fetal bovine serum. Cells were grown at 37°C in a 5% CO_2 incubator. All viruses used for this study were recombinant CVB3 viruses obtained by the transfection of T7 RNA polymerase-generated runoff RNA transcripts from the infectious cDNA clones described below. Virus yields were determined by end-point titration as described previously (30). Virus titers were calculated and expressed as 50% tissue culture infective dose ($TCID_{50}$) values (23).

Plasmids. (i) p53CB3/T7. The CVB3 infectious cDNA clone used for this study was p53CB3/T7, which contains a full-length cDNA of CVB3 (strain Nancy) behind a T7 RNA polymerase promoter. This cDNA clone was constructed by removing the nonviral nucleotides between the T7 promoter and the 5′ end of the CVB3 genome from plasmid pCB3/T7 (14). Furthermore, an MluI site was introduced downstream of the 3′ end of the CVB3 genome to ensure that in vitro-transcribed RNAs did not contain nonviral nucleotides at their 3′ ends, resulting in increased infectivity of the RNA transcripts (data not shown).

(ii) p53CB3-LUC. Plasmid p53CB3-LUC, which contains the firefly luciferase gene in place of the P1 capsid coding region, was derived from pCB3-LUC (30) and contains the same deletion of nonviral nucleotides at the 5′ and 3′ termini as p53CB3/T7.

(iii) pVSVG-GFP. The plasmid pVSVG-GFP (28), which encodes the *ts*045 VSVG protein fused to enhanced green fluorescent protein (EGFP) at its C terminus, was kindly provided by P. Keller and K. Simons (Max Planck Institute of Molecular Biology and Genetics, Dresden, Germany).

(iv) p3A. For construction of the p3A plasmid, the 3A coding sequence was amplified by use of a forward primer that introduced a SalI restriction site and a start codon preceded by a Kozak sequence (p120-4, 5′-GGG GGG TCG ACC ATG GGA CCA CCA GTA TAC AGA-3′ [the SalI site is underlined]) and a reverse primer that introduced a stop codon followed by a BamHI restriction site (p120-5, 5′-GGG GGG GGA TCC CTA TTG AAA ACC CGC AAA GAG-3′ [the BamHI site is underlined]). The PCR product was cloned into pEGFP-C3 (Clontech) from which the EGFP coding region had been deleted.

(v) pC-A1PI-EYFP-S-EGFP-3A. The plasmid pCMS-EGFP (Clontech) was used to express A1PI and 3A from a single plasmid. The pCMS-EGFP plasmid contains two promoters, namely, a cytomegalovirus (CMV) promoter followed by a multiple cloning site and a simian virus 40 (SV40) promoter followed by the EGFP coding sequence. The secretory marker A1PI, with enhanced yellow fluorescent protein (EYFP) at its C terminus, was cloned into the multiple cloning site behind the CMV promoter by the use of EcoRI and NotI. The EGFP coding sequence behind the SV40 promoter was replaced with 3A (wild type or mutant) N-terminally fused to EGFP by the use of AgeI and BclI. The fusion of EGFP to the N terminus of 3A did not affect its protein secretion inhibition function (data not shown).

(vi) pPV5′NC-A1PI-EYFP. For construction of the pPV5′NC-A1PI-EYFP plasmid, the 5′ noncoding region of PV fused to the coding sequence for the secretory marker A1PI was removed from pLink-2B (8) by the use of SmaI and EcoRI and then cloned into pEGFP-C1 (Clontech) by the use of Ecl136III and EcoRI. The A1PI coding sequence was replaced with the coding sequence for A1PI-EYFP by removing A1PI by the use of EcoRV and SmaI and then cloning in the A1PI-EYFP fragment cut with EcoRV and HpaI.

Mammalian two-hybrid plasmids. The pACT, pBIND, and pG5*luc* plasmids were obtained from the Checkmate mammalian two-hybrid system (Promega). For the construction of pACT-3A and pBIND-3A, the 3A coding sequence was cloned into the BamHI and EcoRV sites of the pACT and pBIND plasmids. To obtain pACT and pBIND-3A mutant plasmids, we replaced the wild-type 3A sequence with mutant 3A sequences by using the enzymes Bst1107I and BamHI.

DNA transfections. BGM cell monolayers were grown in 6-well plates (for A1PI secretion assays or Western blot analysis) or on coverslips in 24-well plates (for microscopic purposes) to subconfluence and then transfected with 2 μg of plasmid DNA per well of a 6-well plate or with 0.5 μg of plasmid DNA per well of a 24-well plate. COS cell monolayers were grown in 24-well plates to subconfluence and then transfected with 0.75 μg of plasmid DNA (see below). Transfections were performed by use of the FuGENE 6 reagent (Roche) according to the manufacturer's instructions. Cells were grown at 37°C until further analysis, unless otherwise stated.

VSVG trafficking. The subcellular localization of VSVG-GFP was determined as described previously (5). Briefly, BGM cells expressing either VSVG-GFP alone or VSVG-GFP together with 3A were incubated at 40°C. After a temperature shift to 32°C, the cells were fixed, stained, and analyzed by confocal laser scanning microscopy (CLSM) under a TCS NT microscope (Leica Lasertechnik GmbH, Heidelberg, Germany). Rabbit polyclonal anti-calreticulin was obtained from Sigma-Aldrich. Mouse monoclonal anti-GM130 was obtained from BD. Alexa fluor 594 goat anti-rabbit immunoglobulin G and Alexa fluor 594 goat anti-mouse immunoglobulin G were obtained from Molecular Probes. Primary antibodies were diluted 1:200, and conjugates were diluted 1:500.

A1PI secretion assay. BGM cells grown in six-well plates were transfected with plasmid DNAs, and 20 h after transfection, were washed with phosphate-buffered saline (PBS) and incubated in MEM lacking methionine (Sigma) for 30 min at 37°C. Proteins were pulse labeled with [^{35}S]methionine (50 μCi/well) for 30 min at 37°C and then washed twice with PBS, after which 800 μl of fresh serum-free MEM was added. After a 2-h chase, the medium was collected and adjusted to 1× lysis buffer by the addition of 200 μl of 5× lysis buffer (250 mM Tris [pH 7.4], 750 mM NaCl, 5 mM EDTA, 5% Nonidet P-40, 0.25% sodium dodecyl sulfate [SDS]). The cells were washed twice with PBS and then lysed in 1 ml of lysis buffer (50 mM Tris [pH 7.4], 150 mM NaCl, 1 mM EDTA, 1% Nonidet P-40, 0.05% SDS). An anti-EGFP rabbit polyclonal antiserum (1:1,000) was added to the cell lysate and culture medium, and the mixtures were incubated at 4°C for 16 h. Antibody-protein complexes were collected by the use of protein A-Sepharose (Amersham Biosciences) for 1.5 h, washed twice with dilution buffer (0.01 M Tris [pH 8.0], 0.14 M NaCl, 0.1% bovine serum albumin, 0.1% Triton X-100), once with TSA (0.01 M Tris [pH 8.0], 0.14 M NaCl), and once with 0.05 M Tris (pH 6.8), and then precipitated. The samples were resuspended in 25 μl of Laemmli sample buffer, boiled for 5 min, and analyzed by SDS-polyacrylamide gel electrophoresis (SDS-PAGE). The amounts of radiolabeled A1PI-EYFP in the cell fraction and the medium fraction were quantified by use of a phosphorimaging device (Bio-Rad Multi-Analyst, version 1.0.1).

Site-directed mutagenesis. In vitro mutagenesis was performed with single-stranded DNAs generated from a subgenomic pALTER phagemid construct containing the XhoI (nucleotide [nt] 2014) to SalI (nt 7438) fragment of CVB3 by use of the Altered Sites in vitro mutagenesis system according to the manufacturer's recommendations (Promega). The following synthetic oligonucleotides were used to introduce site-specific mutations (as well as restriction sites, which are underlined, to allow the rapid identification of mutants): primer p388-1, 5′-GAG CAG GTC CGC AAT GGC GGG CGC TGC AGC TGT CTC TGG TGC AAC GCT AAT-3′ (P17A/P18A/P19A mutations, PvuII site); primer p388-12, 5′-CGG TGG TGG TGT CTC AGC TGC AAC GCT AAT TTT-3′ (P14A mutation, PvuII site); primer p388-7, 5′-CAG GTC CGC AAT GGC GGG CGG TGG CGC CGT CTC TGG TGC AAC GCT AAT TTT-3′ (P17A mutation, NarI site); primer p388-8, 5′-GAG CAG GTC CGC AAT GGC GGG CGG CGC CGG TGT CTC TGG TGC AAC GCT AAT-3′ (P18A mutation, NarI site); primer p388-9, 5′-TTT GAG CAG GTC CGC AAT GGC GGG CGC CGG TGG TGT CTC TGG TGC AAC GCT-3′ (P19A mutation, NarI site); primer p388-10, 5′-CGA TTT GAG CAG GTC CGC AAT GGC CGC GGG TGG TGG TGT CTC TGG TGC AAC-3′ (P20A mutation, SacII site); primer p388-11, 5′-CAC AGC CTC ACA GTC TAC CGA TTT GAG CAG GTC CGC AAT GGC GGG CGC TGC AGC TGT CTC TGG TGC AAC GCT AAT-3′ (P17A/P18A/P19A/S31C mutations, PvuII site). The nucleotide sequences of the mutant pALTER clones were verified by sequence analysis. The 3A mutations were introduced into the p53CB3/T7 plasmid by the use of unique BssHII (nt 4242) and BstEII (nt 6263) sites. The mutant cDNAs were used as templates to amplify mutant 3A sequences by use of a forward primer introducing a BamHI site (p120-3, 5′-GAG GCA CGG ATC CAG GGA CCA CCA GTA TAC-3′ [the BamHI site is underlined]) and a reverse primer (p388-6, 5′-GAG GGT GGA GTT GGT CTC CGG AAC CAA CCA TCC-3′) that anneals downstream of the internal ScaI site in the 3A coding sequence. The PCR products were cut with the restriction enzymes BamHI and ScaI and cloned into pEGFP-3A cut with BglII and ScaI to yield the pEGFP-3A mutant plasmids.

Transfection of cells with RNA transcripts. Plasmids were linearized with MluI, purified, and transcribed in vitro by T7 RNA polymerase as described

previously (30). The RNA transcripts were checked by agarose gel electrophoresis. BGM monolayer cells grown to subconfluence in 25-cm^2 flasks were transfected with 2.5 μg of RNA transcripts by the DEAE-dextran method as described previously (30). After transfection, the cells were grown at 37°C. When virus growth was observed, the cultures were incubated until the cytopathic effect (CPE) was complete. In cases in which no CPE was observed after 5 days, the cultures were subjected to three successive cycles of freezing and thawing, and 200 μl was passaged onto fresh BGM monolayer cells, which were grown at 37°C for another 5 days.

Sequence analysis of viral RNA. RNAs were isolated from virus suspensions and reverse transcribed as described previously (30). The 3A coding region was amplified by PCRs with Super*Taq* DNA polymerase (HT Biotechnology), and the sequences were analyzed.

Single-cycle growth analysis. Confluent BGM monolayer cells were infected with virus at a multiplicity of infection (MOI) of 1 $TCID_{50}$ for 30 min at room temperature. The cells were washed three times with PBS, supplied with MEM, and grown at 37°C. At the indicated times, the cells were disrupted by three cycles of freezing and thawing, and the virus titers were determined by end-point titration.

Analysis of viral RNA synthesis. BGM cell monolayers were transfected with 1 μg of T7 RNA polymerase-generated RNA transcripts from MluI-linearized p53CB3/T7-LUC plasmids as described above. At the indicated times posttransfection, the cells were lysed and luciferase activities was assayed as described previously (30).

Calculations. Data are presented as mean values ± standard errors of the means (SEM). Differences were tested for significance by analysis of variance (least significant difference [LSD]).

Western blot analysis. BGM cells grown in six-well plates were transfected with pC-A1PI-EYFP-S-EGFP-3A plasmids (wild type or mutant). At 24 h posttransfection, the cells were lysed in 1× lysis buffer (50 mM Tris [pH 7.4], 150 mM NaCl, 1 mM EDTA, 1% Nonidet P-40, 0.05% SDS). Samples were run in an SDS–12.5% polyacrylamide gel and transferred to a nitrocellulose membrane (Bio-Rad). EGFP fusion proteins were stained with an anti-EGFP polyclonal antiserum (diluted 1:10,000) and peroxidase-conjugated goat anti-rabbit immunoglobulins (diluted 1:5,000) and visualized with the Lumi-Light^{plus} Western blotting substrate (Roche Molecular Biochemicals) according to the manufacturer's instructions.

Mammalian two-hybrid analysis. COS cells grown in 24-well plates were transfected with a total of 0.75 μg of plasmid DNA (1:1:1 mix of the pACT, pBIND, and pG5*luc* plasmids). At 48 h posttransfection, the cells were lysed, and both the firefly luciferase and *Renilla* luciferase enzyme activities were measured from the same cell lysate by use of a dual-luciferase reporter assay system (Promega) as described previously (4). An analysis of the *Renilla* luciferase activities, encoded by the pBIND plasmid and allowing monitoring of the transfection efficiency, revealed no gross differences in efficiencies of transfection among the different samples.

RESULTS

Inhibition of ER-to-Golgi transport by CVB3 and 3A expression. To monitor secretory pathway trafficking, we made use of a GFP fusion of the temperature-sensitive *ts*045 mutant of VSVG, a well-known membrane-bound secretory marker (VSVG-GFP). Figure 1A shows that at the nonpermissive temperature (40°C), VSVG-GFP was improperly folded and, as a consequence, retained in the ER (as indicated by its colocalization with calreticulin, an ER protein). Upon shifting the temperature to the permissive temperature (32°C), the protein was correctly folded and transported out of the ER. After 45 min, the majority of the protein was found at the Golgi complex (as indicated by its colocalization with GM130, a *cis*-Golgi protein) (Fig. 1B). After 120 min, the protein was localized mostly at the plasma membrane (Fig. 1C).

To investigate whether CVB3 inhibits vesicular trafficking, we transfected BGM cells with the VSVG-GFP expression plasmid, incubated them at 40°C, and then infected them with CVB3 at an MOI of 50. The infected cells were further incubated at 40°C and then shifted to 32°C (for 120 min) at 1-h time intervals between 0 and 5 h postinfection (p.i.). The cells were fixed and stained, and VSVG-GFP localization was analyzed by CLSM. In infected cells that were kept at 40°C, VSVG-GFP was retained in the ER (Fig. 1D). In infected cells that were shifted to 32°C at 0, 1, 2, or 3 h p.i., VSVG-GFP was mainly localized at the plasma membrane (similar to the case shown in Fig. 1C). In cells that were shifted to 32°C at 4 or 5 h p.i., VSVG-GFP was found to accumulate in both the ER (Fig. 1E) and a dispersed post-ER compartment that also contained the *cis*-Golgi marker (Fig. 1F). Together, these results suggest that in CVB3-infected cells, protein transport is blocked from about 4 h p.i. at a step between the ER and the Golgi.

Next, we tested whether expression of the CVB3 3A protein alone was sufficient to inhibit ER-to-Golgi transport. BGM cells were cotransfected with VSVG-GFP and a 3A expression plasmid (at a 1:3 ratio to optimize the cotransfection efficiency). The cells were incubated at 40°C for 20 h (Fig. 1G) and then shifted to 32°C for 120 min. Figures 1H and I show that in cells cotransfected with VSVG-GFP and 3A, VSVG was mainly retained in the ER (Fig. 1H) and in a dispersed post-ER compartment that also contained the *cis*-Golgi marker (Fig. 1I), which was more or less similar to the case for infected cells.

In order to quantify the inhibitory effects of CVB3 infection and 3A expression on protein secretion, we made use of the reporter protein A1PI, a secreted soluble glycoprotein. In pulse-chase experiments, the level of A1PI secretion can be determined by measuring the percentages of reporter protein in the cell and medium fractions. For this study, a fusion protein of A1PI and EYFP was used because the A1PI protein was found to migrate to the same position as a nonspecific protein band in BGM cell lysates (data not shown). Figure 2A shows that the A1PI-EYFP fusion protein, which was labeled for a 30-min pulse period and immunoprecipitated with anti-EGFP, was efficiently secreted into the medium during a 2-h chase period.

The inhibitory effect of CVB3 infection on protein secretion was determined at various times p.i. Because enterovirus infection shuts off cap-dependent translation (9), a plasmid was used that contained the A1PI coding sequence behind the PV 5′ noncoding region. Cells transfected with this construct were infected with CVB3 (MOI = 50), pulse labeled for 30 min with [^{35}S]methionine at 2, 4, or 6 h p.i., and subsequently chased for 2 h in the presence of unlabeled methionine. In cells labeled at 2 h p.i. (i.e., chased between 2.5 and 4.5 h p.i.), the majority of A1PI was secreted into the medium (Fig. 2A). In cells labeled at 4 or 6 h p.i. (i.e., chased between 4.5 and 6.5 h p.i. and between 6.5 and 8.5 h p.i., respectively), however, only a small amount of A1PI was observed in the medium fraction, whereas a large amount of A1PI was retained in the cell. The amount of A1PI in the medium fraction was determined as the percentage of the total amount of A1PI and compared to that of control cells (for which the value was normalized to 100% A1PI secretion). The average results of three independent experiments are shown in Fig. 2B. The results demonstrate that CVB3 infection inhibited reporter protein secretion to approximately 30% compared to control cells from about 4 h p.i.

To quantify the inhibitory effect of 3A on protein secretion, we coexpressed the 3A protein (behind an SV40 promoter)

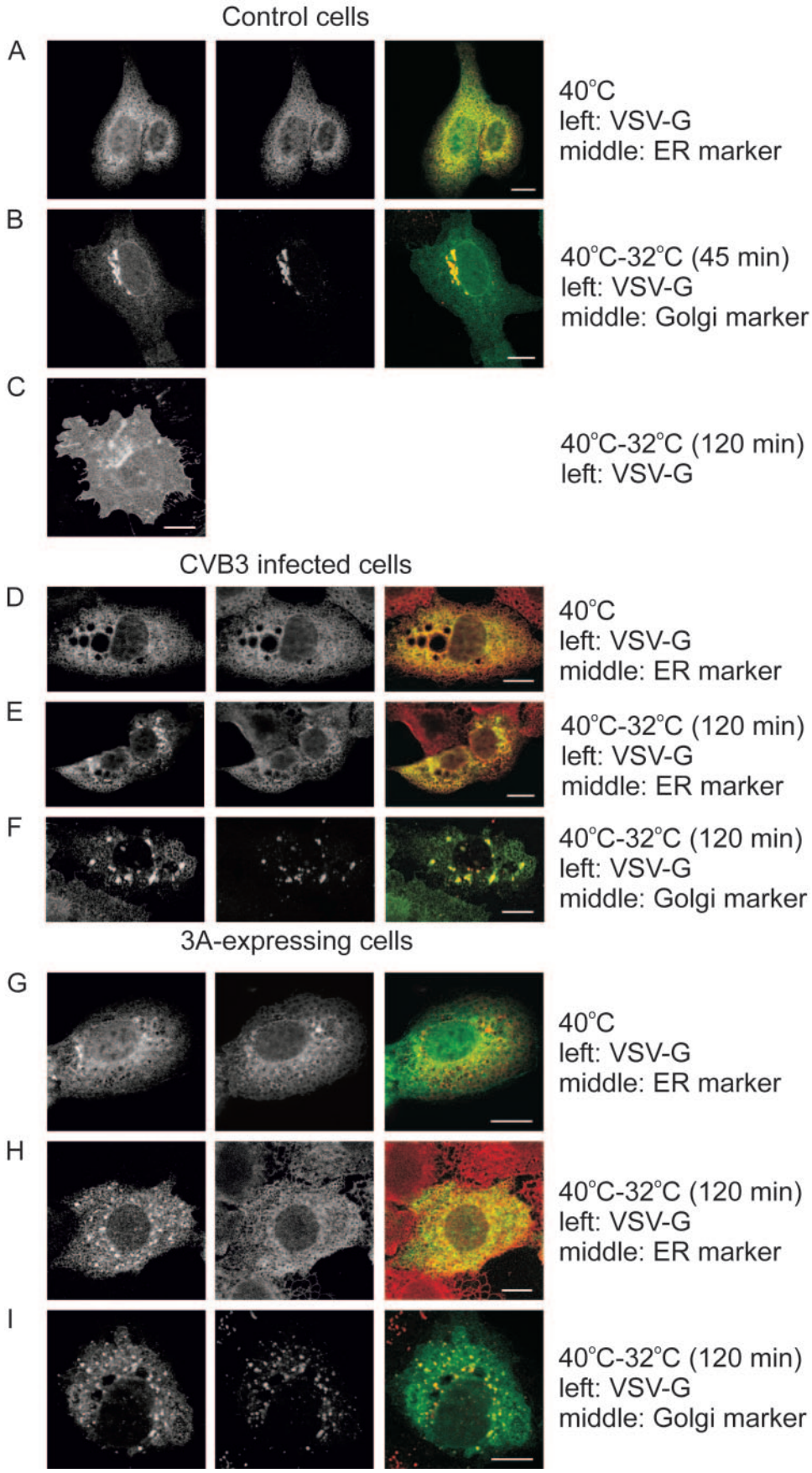

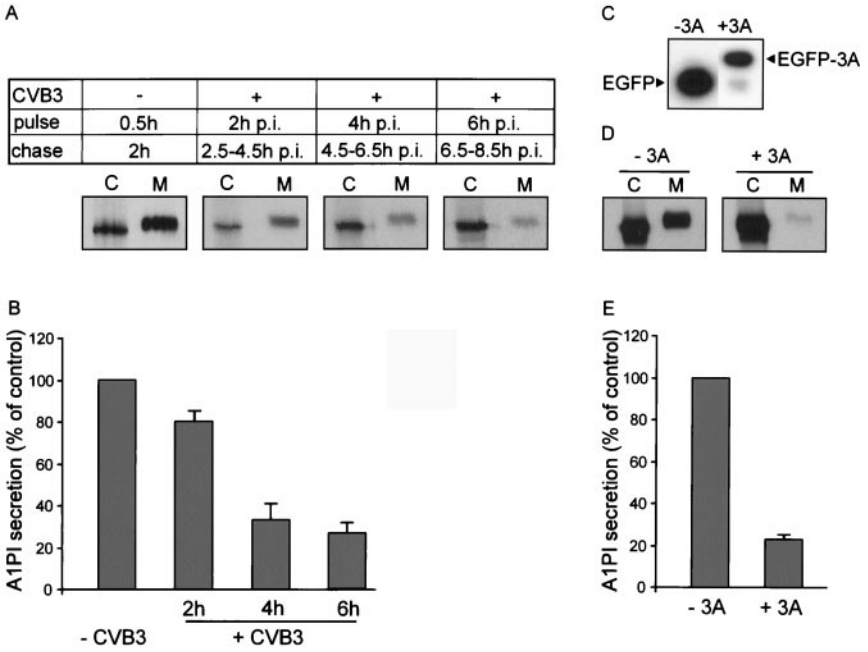

FIG. 2. CVB3 infection (MOI of 50) and expression of the 3A protein inhibit A1PI secretion. BGM cells were transfected with A1PI expression constructs. Twenty hours after transfection, the cells were starved of methionine for 30 min, labeled with [^{35}S]methionine for 30 min, and then chased for 2 h. Cell (C) and medium (M) fractions were collected and analyzed for the amount of labeled reporter protein by immunoprecipitation with an anti-EGFP antiserum, SDS-PAGE, and phosphorimaging. (A) Cells transfected with a plasmid containing A1PI behind the PV noncoding region were infected and subjected to pulse-chase analysis at 2, 4, and 6 h p.i. The differences in migration between A1PI in the medium and cell fractions were due to differences in the glycosylation state (endoglycosidase F treatment resulted in faster migration of A1PI in both the medium and cell fractions [data not shown]). (B) Average secretion (means ± standard errors of the means [SEM]) of three independent experiments. A1PI secretion was calculated as the percentage of A1PI secretion in uninfected control cells, which was normalized to 100%. (C to E) BGM cells were transfected with constructs expressing either EGFP (−3A) or EGFP-3A (+3A) from an SV40 promoter and the A1PI-EYFP protein from a cytomegalovirus promoter. (C) Western blot analysis of EGFP and EGFP-3A expression. (D) Analysis of A1PI secretion. (E) Average secretion (means ± SEM) of three independent experiments. A1PI secretion was calculated as the percentage of A1PI secretion in EGFP-expressing control cells, which was normalized to 100%.

and the A1PI secretion marker (behind a CMV promoter) from a single plasmid. The 3A protein was expressed as an EGFP-3A fusion protein (the fusion of EGFP to the N terminus of 3A did not affect its protein secretion inhibition function [data not shown]). As a control, a plasmid was constructed that contained the EGFP sequence behind the SV40 promoter. Western blot analysis showed that both proteins were efficiently expressed (Fig. 2C). Figure 2D shows that the expression of the 3A protein resulted in a severely reduced amount of labeled reporter protein in the medium fraction. A quantitative analysis of A1PI secretion in three independent experiments showed that 3A expression inhibited reporter protein secretion to approximately 25% of that of control cells (Fig. 2E) (the percentage of A1PI secretion was calculated as described above).

Importance of proline-rich region in 3A for inhibition of ER-to-Golgi transport. The enterovirus and rhinovirus 3A proteins are characterized by the presence of a proline-rich region in the N terminus (Fig. 3). This proline-rich region is located at aa 17 to 19 (numbering refers to the CVB3 3A protein). Pro^{17} and Pro^{19} are present in all 63 enterovirus and rhinovirus 3A proteins that have been sequenced to date (except for enterovirus [EV] type 71). Pro^{18} is present in nearly all enteroviruses and rhinoviruses (except for coxsackievirus A16 [CVA16], CVA24, EV70, and EV71). All human enterovirus group B (HEV-B) members (which include all CVB types, all echovi-

FIG. 1. CVB3 infection and expression of the 3A protein inhibit VSVG-GFP trafficking. BGM cells were transfected with a construct coding for the GFP-tagged *ts*045 temperature-sensitive mutant of the VSVG protein, either alone or together with 3A, and grown at 40°C for 20 h. (A to C) Control cells. In control cells, VSVG was improperly folded at 40°C, and as a consequence, was retained in the ER, as shown by its colocalization with calreticulin (merged picture on the right in panel A). Upon shifting to the permissive temperature (32°C), the VSVG-GFP protein was correctly folded and transported out of the ER. VSVG could be observed in the Golgi complex after 45 min, as shown by its colocalization with GM130, a *cis*-Golgi marker (B), and at the plasma membrane after 120 min (C). (D to F) Cells infected with CVB3 (MOI of 50) for 5 h at 40°C. At 40°C, VSVG was retained in the ER (D). Upon shifting to 32°C for 120 min, VSVG could be found in the ER (E) and a post-ER compartment that also contained the *cis*-Golgi marker (F). (G to H) 3A-expressing cells. VSVG was retained in the ER at 40°C (G), whereas it was observed in the ER (H) and a post-ER compartment that also contained the *cis*-Golgi marker (I) when shifted to 32°C for 120 min. Bar = 10 μm.

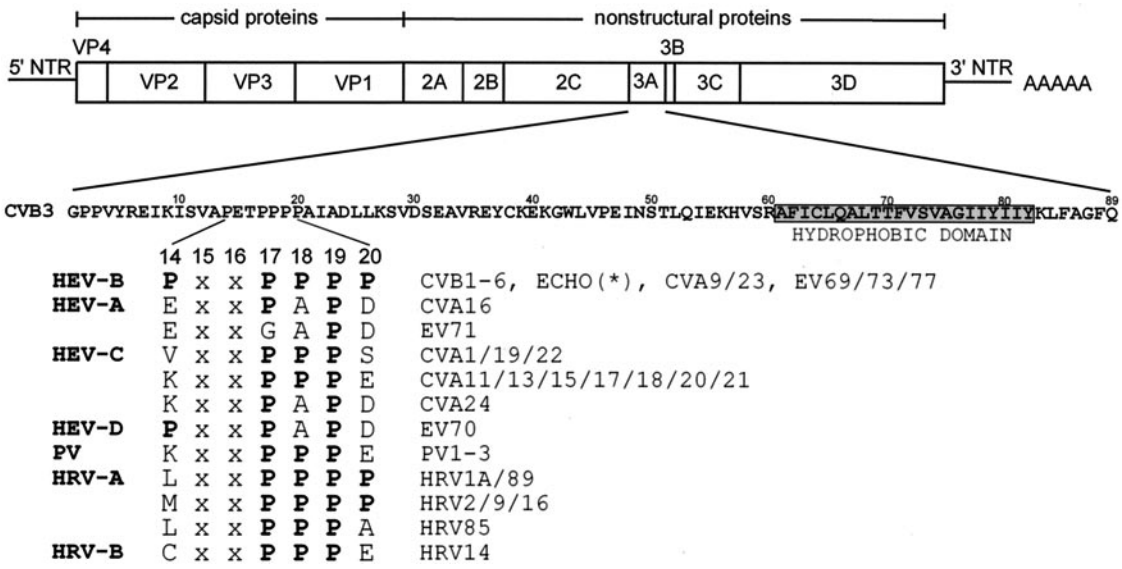

FIG. 3. Alignment of aa 14 to 20 of the enterovirus and rhinovirus 3A proteins. The genome organization of CVB3 is depicted. CVB3 contains a single open reading frame flanked by a 5′ and 3′ nontranslated region (NTR) and a poly(A) tail. The four capsid proteins (VP1 to VP4) and seven nonstructural proteins (2A, 2B, 2C, 3A, 3B, 3C, and 3D) are shown. The 3A protein of CVB3 is an 89-aa protein which contains a C-terminal hydrophobic domain (aa 61 to 82). 3A contains several Pro residues (at positions 14 and 17 to 20) in its N terminus. An alignment of these residues for all enteroviruses and rhinoviruses that have been sequenced to date is shown. The species names are shown in bold. HEV-B, human enterovirus B; HEV-A, human enterovirus A; HEV-C, human enterovirus C; HEV-D, human enterovirus D; PV, poliovirus; HRV-A, human rhinovirus A; HRV-B, human rhinovirus B; CVB, coxsackievirus B; ECHO(*), all echoviruses sequenced to date (i.e., echoviruses 1 to 7, 9, 11 to 21, 24 to 27, and 29 to 33); CVA, coxsackievirus A; EV, enterovirus.

ruses, some CVA types, and several unassigned EVs) contain additional Pro residues at positions 14 and 20.

Proline-rich regions are often involved in protein-protein interactions (reviewed in reference 13). To investigate the functional importance of the proline-rich region in the CVB3 3A protein, we constructed mutant 3A expression plasmids. Since Pro^{17}, Pro^{18}, and Pro^{19} are the most conserved proline residues, we first replaced these three residues simultaneously with Ala residues (P17A/P18A/P19A). Figures 4A and B show that this 3A mutant was no longer able to inhibit protein secretion. This was not due to reduced expression of the mutant protein, as it was expressed at a similar level as wild-type 3A (Fig. 4E). Moreover, in cells that coexpressed this mutant 3A protein and VSVG-GFP, we observed that VSVG accumulated at the plasma membrane (data not shown). Thus, the proline-rich region is required for the ability of 3A to inhibit protein secretion.

To investigate the importance of the Pro residues individually, we constructed mutant 3A proteins in which single Pro residues at positions 14, 17, 18, 19, and 20 were replaced with Ala residues (mutations P14A, P17A, P18A, P19A, and P20A, respectively). The P19A mutation completely abolished the ability of 3A to inhibit A1PI secretion (to a similar extent as the P17A/P18A/P19A mutant) (Fig. 4C and D). The P14A, P17A, and P20A mutations also impaired the ability of 3A to inhibit protein secretion, although to a lesser extent. The P18A mutation had no effect on the secretion inhibition activity of 3A. Western blot analysis showed that all mutant 3A proteins were efficiently expressed (Fig. 4E). Thus, the Pro residues at positions 14, 17, 19, and 20, but not that at position 18, are important for the ability of 3A to inhibit protein secretion.

Importance of proline-rich region in 3A for its function in viral replication. To study the effect of 3A mutations on viral RNA replication and virus growth, we introduced mutations into an infectious cDNA clone of CVB3. For each mutation, two p53CB3/T7 clones were tested, derived from two independently generated site-directed mutagenesis clones. The effects of the P17A/P18A/P19A, P14A, P17A, P18A, P19A, and P20A mutations on virus viability were studied by the transfection of BGM cells with RNA transcripts. The results obtained for the P17A/P18A/P19A mutant are described below. Cells transfected with RNA transcripts carrying single Pro mutations exhibited complete CPE in all transfections (Fig. 5A). vRNAs were isolated from these cell cultures, and the 3A coding region was amplified by reverse transcription-PCR and then sequenced. In all cases, the original mutations were retained in the vRNAs, and no secondary amino acid replacements had occurred. The mutant viruses were further characterized by single-cycle growth analysis (Fig. 5B). Viruses carrying mutations exhibited wild-type growth characteristics. This indicated that the mutant 3A proteins were correctly folded. In conclusion, mutation of the individual Pro residues had no effect on viral replication.

Identification of a second-site suppressor mutation. Cells transfected with RNA transcripts containing the P17A/P18A/P19A mutations exhibited no CPE up to 5 days posttransfection. After passage to fresh BGM cells, CPE was observed in only one of eight transfected cell cultures (Fig. 6A). A sequence analysis of the 3A coding region showed that the introduced mutations were retained in the obtained virus but that a second-site suppressor mutation, A→T, had occurred at nt 5119. This nucleotide mutation resulted in a Ser-to-Cys

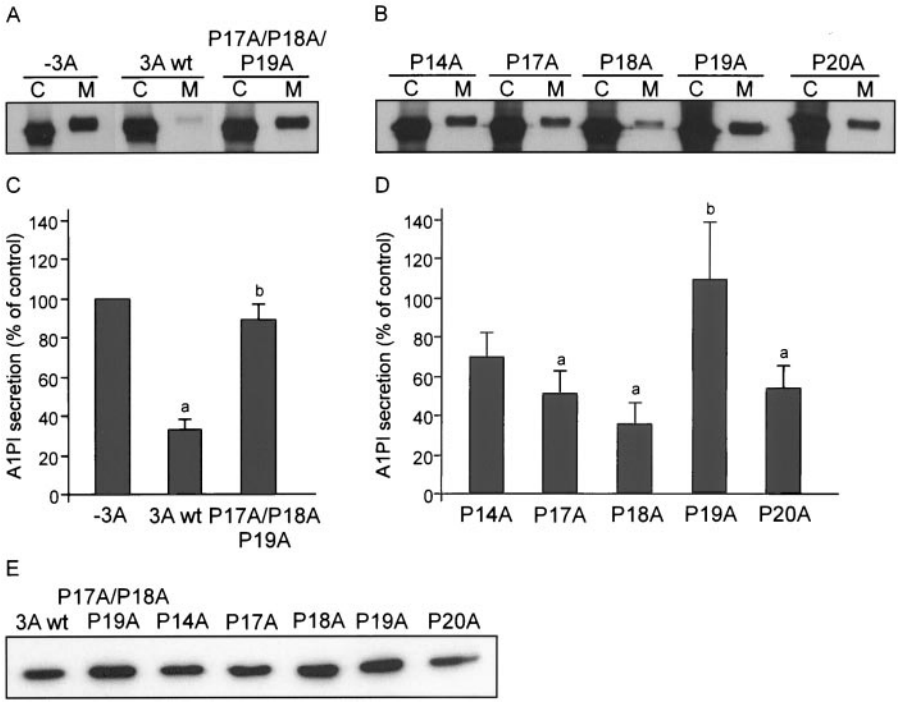

FIG. 4. Proline-rich region is required for secretion inhibition by CVB3 3A. Cells were transfected with plasmids expressing the indicated 3A mutant proteins from an SV40 promoter and the A1PI reporter protein from a cytomegalovirus promoter. Twenty hours after transfection, the cells were labeled with [^{35}S]methionine for 30 min and chased in the presence of unlabeled methionine for 2 h. Cell (C) and medium (M) fractions were collected, immunoprecipitated with an anti-EGPF serum, analyzed by SDS-PAGE (A and C), and quantified by phosphorimaging (B and D). The amount of secreted A1PI in the absence of 3A was normalized to 100%, and the ability of 3A and 3A mutants to secrete A1PI was calculated as a percentage of the A1PI secretion in control cells without 3A. Values represent means ± SEM of three independent experiments. a, significantly different from A1PI secretion in control cells without 3A; b, significantly different from A1PI secretion in the presence of wild-type 3A (calculated by analysis of variance with LSD; $P < 0.05$). (E) Western blot of EGFP-3A wild-type and mutant proteins.

substitution at aa 31 of the 3A protein. To demonstrate that this amino acid change in 3A was indeed responsible for the growth of this mutant virus, we introduced the P17A/P18A/P19A/S31C mutations into the infectious cDNA clone. BGM cells transfected with RNA transcripts of this mutant showed CPE on all occasions. A sequence analysis of the 3A coding regions of the resulting viruses showed that the introduced mutations were retained in the vRNAs. Thus, a S31C mutation can indeed rescue the defect in virus growth caused by the P17A/P18A/P19A mutations. Single-cycle growth analysis showed that the mutant virus exhibited a severe delay in virus growth (Fig. 6B).

To investigate whether the quasi-infectious phenotype [a definition that indicates that the mutation disrupts vRNA replication to such an extent that (pseudo)reversion mutations or second-site suppressor mutations can arise but that no virus progeny can be observed harboring the original mutation] of the P17A/P18A/P19A mutant was due to a defect in polyprotein processing, we performed in vitro translation reactions with RNA transcripts generated from the wild type and the mutant cDNA clone. An analysis of the [^{35}S]methionine-labeled translation products by SDS-PAGE showed no differences between the wild type and the mutant, arguing that it is unlikely that the growth defect of the mutant was due to aberrant processing of the viral polyprotein (data not shown). To investigate whether the primary defect occurred at the level of vRNA replication, we introduced the P17A/P18A/P19A mutations into p53CB3/T7-LUC, a subgenomic replicon that contains the luciferase gene in place of the P1 coding region. BGM cells were transfected with RNA transcripts of this clone, and at 10 h posttransfection, the cells were lysed and luciferase expression was analyzed. Transfected cells were grown in the absence or presence of guanidine hydrochloride (GuHCl), an inhibitor of enterovirus replication that is used to determine luciferase levels in the absence of replication (under this condition, luciferase production only reflects translation of the transfected replicon RNA). Figure 6C shows that luciferase production by replicons carrying the P17A/P18A/P19A mutant was the same in the absence or presence of GuHCl and also the same as that observed for wild-type replicons when replication was inhibited by GuHCl. However, replicons carrying the P17A/P18A/P19A/S31C mutant showed an increase in luciferase production. These findings provide evidence that the quasi-infectious phenotype of the P17A/P18A/P19A mutant was due to a primary defect in vRNA replication.

We also investigated whether the second-site suppressor mutation could rescue the effect of the P17A/P18A/P19A mutant on protein secretion. To this end, we introduced the P17A/P18A/P19A and S31C mutations into the 3A protein and tested their effect on A1PI secretion as described above. The P17A/P18A/P19A/S31C mutant caused a similar disruptive effect on the ability of 3A to inhibit A1PI secretion as the

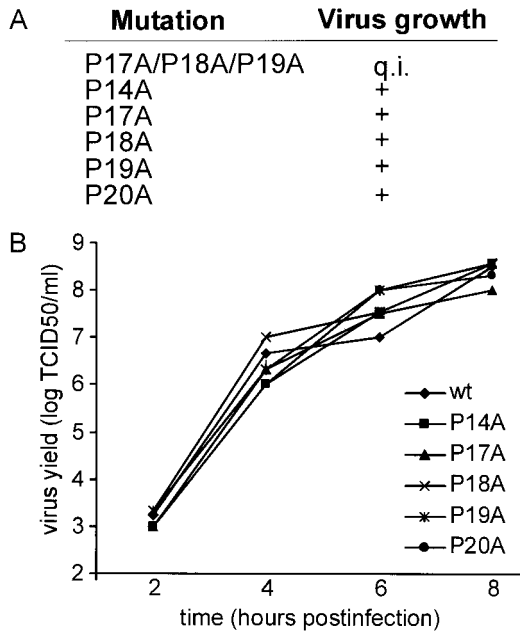

FIG. 5. Proline-rich region is not important for CVB3 growth. (A) Effect of the indicated 3A mutations on virus growth. Mutations were introduced into the infectious cDNA clone p53CB3/T7. Copy RNA transcripts were transfected into BGM cells and examined for the ability to yield viruses. All mutations resulted in viable viruses except the P17A/P18A/P19A mutations, which caused a quasi-infectious (q.i.) phenotype. (B) Single-cycle growth analysis of mutant viruses. BGM cells were infected at an MOI of 1 and incubated at 37°C. At 2, 4, 6, or 8 h postinfection, viruses were released from the infected cells by three cycles of freezing and thawing. Virus titers were determined by titration on BGM cells and expressed in $TCID_{50}$ values.

P17A/P18A/P19A mutant (Fig. 6D). Thus, the second-site suppressor mutation S31C did not rescue the defect in protein secretion inhibition caused by the P17A/P18A/P19A mutations.

It has been suggested that the enterovirus 3A protein forms a homodimer. Cross-linking and analytical ultracentrifugation studies showed that the first 60 aa of the PV 3A protein form a homodimer (26). Evidence for PV 3A homomultimerization was also obtained by yeast two-hybrid analysis (34). The possibility was considered that the second-site suppressor mutation S31C might restore 3A-3A interactions that were disrupted by the P17A/P18A/P19A mutations. We investigated homomultimerization reactions of CVB3 wild-type 3A and 3A proteins carrying the P17A/P18A/P19A or P17A/P18A/P19A/S31C mutations by use of a mammalian two-hybrid system (4). To this end, we cloned the 3A sequences in the correct reading frame into the expression plasmids pACT (which provides the activation domain of herpes simplex virus type 1 VP16) and pBIND (which provides the yeast Gal4 DNA binding domain). COS cells were cotransfected with these two plasmids and with the plasmid pG5*luc*, a reporter plasmid that contains five GAL4 binding sites upstream of a minimal TATA box that precedes the firefly luciferase gene. An analysis of the luciferase activity showed that the wild-type CVB3 3A protein did indeed form homomultimers (Fig. 6E). No multimerization was observed with 3A carrying the P17A/P18A/P19A mutations. No obvious increase in multimerization was observed with 3A carrying mutation P17A/P18A/P19A/S31C.

DISCUSSION

In this study, we showed that CVB3 infection and expression of the 3A protein alone interfere with protein secretion by blocking ER-to-Golgi transport. Moreover, we demonstrated that the proline-rich region in the N terminus of 3A is required for this ability. Pro^{17}, Pro^{18}, and Pro^{19} are evolutionarily conserved in nearly all enteroviruses and rhinoviruses. Of these residues, Pro^{19} was found to be the most important for 3A to inhibit protein secretion. Mutation of this residue almost completely abolished this activity. The mutation of Pro^{17}, on the other hand, was far less disruptive for the inhibitory activity of 3A. Mutation of this residue was even less disruptive than mutations of the less-conserved Pro^{14} and Pro^{20} residues, which are conserved in all HEV-B members (i.e., all CVBs and echoviruses, some CVAs, and some unnamed enteroviruses) but not in other enteroviruses and rhinoviruses. Remarkably, the mutation of Pro^{18} had no notable effect.

The mechanism by which 3A inhibits protein secretion is still unknown. Therefore, we can only speculate about a role of the proline-rich region in the inhibition of protein secretion. Pro residues can play an important role in protein-protein interactions (reviewed in reference 32). We propose that the 3A protein exerts its activity by tethering a cellular protein through an interaction with its proline-rich region.

Two well-known protein interaction domains that interact with Pro residues are Src homology 3 (SH3) and WW domains. SH3 domains recognize proline-rich sequences containing the core PXXP, where "X" denotes any amino acid. WW domains bind ligands containing PPXY or PPLP core motifs, usually flanked by additional Pro residues (13, 17). It seems unlikely, however, that 3A interacts with proteins containing an SH3 or a WW domain. When considering putative interaction domains, one should take into account the fact that the Pro^{14} and Pro^{20} residues are not conserved among all enteroviruses and rhinoviruses. The 3A proteins of CVB3 and PV (which lacks Pro^{14} and Pro^{20}) most likely use identical mechanisms to inhibit protein secretion. Given the observation that a mutation of Pro^{18} had little effect on this ability, these proteins most likely only share Pro^{17} and Pro^{19} for their secretion inhibition function. Therefore, alternative interaction domains or mechanisms should be considered.

Recently, the structure of the first 60 aa of the PV 3A protein was determined by nuclear magnetic resonance spectroscopy (26). The PV 3A protein was found to form a classic homodimer. Dimerization occurs through ionic interactions, hydrogen bonds, and hydrophobic interactions between two helices formed by aa 23 to 29 and aa 32 to 41. Figure 7 shows the putative structure of the first 60 aa of CVB3, obtained by molecular modeling of the published PV 3A structure. The structure suggests that the proline-rich regions of two interacting 3A proteins are oriented in such a way that they are contiguous and thereby form a Pro platform. We suggest that this Pro platform, rather than specific SH3 or WW binding domains, may be the interaction domain responsible for the binding of a (still unknown) cellular protein.

The CVB3 3A protein inhibited protein secretion to an

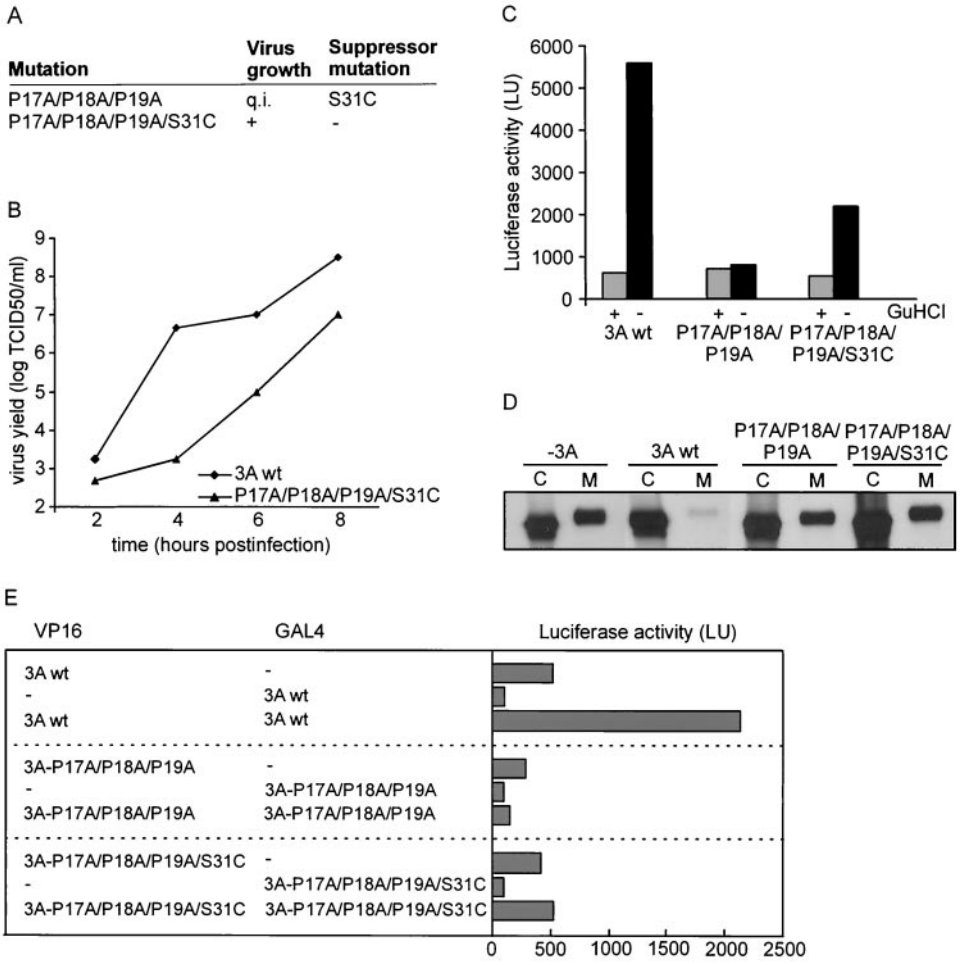

FIG. 6. A second-site suppressor mutation in 3A rescues the effect of the P17A/P18A/P19A mutations. (A) Effect of the indicated 3A mutations on virus growth. The P17A/P18A/P19A mutations resulted in a quasi-infectious (q.i.) phenotype and yielded virus in only one of eight transfected cultures. A sequence analysis showed the presence of the second-site suppressor mutation S31C. The P17A/P18A/P19A/S31C mutant yielded virus upon all transfections. (B) Effect of the P17A/P18A/P19A/S31C mutations on virus growth. Single-cycle growth analysis was performed as described in the legend to Fig. 5. (C) Effect of P17A/P18A/P19A and P17A/P18A/P19A/S31C mutations on viral RNA replication. The mutations were introduced into p53CB3-LUC, and transcripts from these replicons were transfected into BGM cells. The cells were grown for 10 h in the presence (+) or absence (−) of 2 mM GuHCl, an inhibitor of enterovirus replication. Luciferase activities are depicted in light units (LU). (D) Effect of P17A/P18A/P19A and P17A/P18A/P19A/S31C mutations on A1PI secretion. The analysis was performed as described in the legend to Fig. 4. (E) Homomultimerization reactions of wild-type 3A and the 3A-P17A/P18A/P19A and 3A-P17A/P18A/P19A/S31C mutants expressed as fusion proteins to the HSV VP16 activation domain or the yeast GAL4 DNA binding domain. COS cells were transfected with the indicated constructs and assayed for firefly luciferase production at 48 h posttransfection. Dashes indicate the expression of unfused VP16 or GAL4 protein. LU, light units.

extent similar to that previously described for the 3A protein of the closely related PV (7). A PV mutant (mutant 3A-2) containing a Ser insertion between 3A residues 14 and 15 (corresponding to aa 15 and 16 in CVB3) was strongly impaired in inhibiting A1PI secretion (7). The PV carrying this insertion mutation showed a reduced ability to inhibit the presentation of MHC I-antigen complexes (3) and to block the secretion of cytokines and interleukins (6). The introduction of this mutation into CVB 3A (i.e., a Ser insertion between residues 15 and 16) also interfered with the ability of 3A to inhibit A1PI secretion (data not shown). The mutation disrupted this 3A function to a similar extent as the P19A mutation. It is therefore reasonable to assume that CVB3 carrying Pro-to-Ala mutations (in particular P19A) is also impaired in the ability to suppress MHC I-antigen presentation and to block the secretion of cytokines and interleukins.

Enterovirus genome replication takes place at secretory pathway-derived membrane vesicles that accumulate in the cytosol of the infected cell. The 2BC protein has been identified as playing a major role in the accumulation of these vesicles (2, 24, 25). It has been speculated that the 3A-induced inhibition of ER-to-Golgi transport might also contribute to the accumulation of the vesicles with which the viral replication complexes are associated (27). However, in the present study, we showed that viruses carrying mutations in 3A that interfered with its ability to inhibit ER-to-Golgi transport replicated with wild-type growth characteristics, arguing against a possible role of 3A in the accumulation of replication vesicles. It

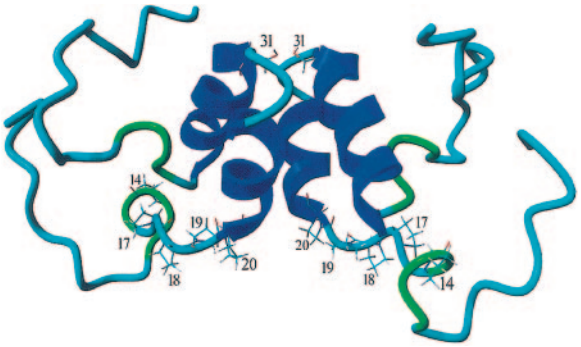

FIG. 7. Putative model of CVB3 3A protein. The structural model shows a homodimer of the N-terminal 60 aa of CVB3 3A. Molecular modeling (using WHATIF [31] and YASARA NOVA [15] software) was used to predict the CVB3 3A structure on the basis of the published nuclear magnetic resonance structure of the N-terminal 60 aa of PV 3A. Pro^{14}, Pro^{17}, Pro^{18}, Pro^{19}, and Pro^{20} at the bottom of the 3A dimer and Ser^{31} in the loop connecting the two α-helices are indicated.

cannot be excluded that the 3A protein contributes to an accumulation of vesicles, but this activity does not seem to be essential for viral RNA replication, at least not in vitro.

In contrast to the wild-type phenotype of viruses carrying the single Pro-to-Ala mutations, the P17A/P18A/P19A mutant yielded a quasi-infectious phenotype. Upon multiple RNA transfections, only on one occasion was virus obtained. A sequence analysis of the viral RNA showed that a second-site suppressor mutation at position 31 of 3A (S31C) had occurred. This second-site suppressor mutation rescued a defect in 3A in viral RNA replication, but not its ability to inhibit protein secretion. Since the single Pro-to-Ala mutations did not affect viral RNA replication, it can be hypothesized that the P17A/P18A/P19A mutations interfere with the conformation of 3A or its precursor 3AB and thereby with its function in vRNA replication. Indeed, we found that the P17A/P18A/P19A mutation interfered with 3A homomultimerization in a mammalian two-hybrid system. This finding is remarkable because the structural model predicts no important role for the proline-rich region in dimerization. Together, these data are consistent with the idea that the P17A/P18A/P19A mutation causes a general disruption of the 3A structure. How the S31C suppressor mutation, which is present in the loop between the two α-helices implicated in dimerization (Fig. 7), can (partially) rescue the defect in vRNA replication imposed by the P17A/P18A/P19A mutation remains to be established. Further research is needed to establish the requirement of 3A dimerization for its function in vRNA replication and its ability to inhibit ER-to-Golgi trafficking.

ACKNOWLEDGMENTS

We thank Jeroen van Kilsdonk, Vladimir van Hoek, and Sander Jannink for technical assistance, Henri Dijkman for assistance with CLSM, and Patrick Keller and Kai Simons (Max Planck Institute of Molecular Biology and Genetics, Dresden, Germany) for the kind gift of the VSVG-GFP plasmid.

This work was partly supported by grants from The Netherlands Organization for Scientific Research (NWO-VIDI-917.46.305), the M. W. Beijerink Virology Fund from the Royal Netherlands Academy of Sciences, and the European Communities (INTAS 2012).

REFERENCES

1. **Bernstein, H. D., P. Sarnow, and D. Baltimore.** 1986. Genetic complementation among poliovirus mutants derived from an infectious cDNA clone. J. Virol. **60:**1040–1049.
2. **Bienz, K., D. Egger, and T. Pfister.** 1994. Characteristics of the poliovirus replication complex. Arch. Virol. **9**(Suppl.)**:**147–157.
3. **Deitz, S. B., D. A. Dodd, S. Cooper, P. Parham, and K. Kirkegaard.** 2000. MHC I-dependent antigen presentation is inhibited by poliovirus protein 3A. Proc. Natl. Acad. Sci. USA **97:**13790–13795.
4. **de Jong, A. S., I. W. Schrama, P. H. Willems, J. M. Galama, W. J. Melchers, and F. J. Van Kuppeveld.** 2002. Multimerization reactions of coxsackievirus proteins 2B, 2C and 2BC: a mammalian two-hybrid analysis. J. Gen. Virol. **83:**783–793.
5. **de Jong, A. S., E. Wessels, H. B. P. M. Dijkman, J. M. D. Galama, W. J. G. Melchers, P. H. M. G. Willems, and F. J. M. van Kuppeveld.** 2003. Determinants for membrane association and permeabilization of the coxsackievirus 2B protein and the identification of the Golgi complex as the target organelle. J. Biol. Chem. **278:**1012–1021.
6. **Dodd, D. A., T. H. Giddings, Jr., and K. Kirkegaard.** 2001. Poliovirus 3A protein limits interleukin-6 (IL-6), IL-8, and beta interferon secretion during viral infection. J. Virol. **75:**8158–8165.
7. **Doedens, J. R., T. H. Giddings, Jr., and K. Kirkegaard.** 1997. Inhibition of endoplasmic reticulum-to-Golgi traffic by poliovirus protein 3A: genetic and ultrastructural analysis. J. Virol. **71:**9054–9064.
8. **Doedens, J. R., and K. Kirkegaard.** 1995. Inhibition of cellular protein secretion by poliovirus proteins 2B and 3A. EMBO J. **14:**894–907.
9. **Ehrenfeld, E.** 1982. Poliovirus-induced inhibition of host-cell protein synthesis. Cell **28:**435–436.
10. **Giachetti, C., S. S. Hwang, and B. L. Semler.** 1992. *cis*-Acting lesions targeted to the hydrophobic domain of a poliovirus membrane protein involved in RNA replication. J. Virol. **66:**6045–6057.
11. **Harris, K. S., W. Xiang, L. Alexander, W. S. Lane, A. V. Paul, and E. Wimmer.** 1994. Interaction of poliovirus polypeptide 3CDpro with the 5′ and 3′ termini of the poliovirus genome. Identification of viral and cellular cofactors needed for efficient binding. J. Biol. Chem. **269:**27004–27014.
12. **Hope, D. A., S. E. Diamond, and K. Kirkegaard.** 1997. Genetic dissection of interaction between poliovirus 3D polymerase and viral protein 3AB. J. Virol. **71:**9490–9498.
13. **Kay, B. K., M. P. Williamson, and M. Sudol.** 2000. The importance of being proline: the interaction of proline-rich motifs in signaling proteins with their cognate domains. FASEB J. **14:**231–241.
14. **Klump, W. M., I. Bergmann, B. C. Muller, D. Ameis, and R. Kandolf.** 1990. Complete nucleotide sequence of infectious coxsackievirus B3 cDNA: two initial 5′ uridine residues are regained during plus-strand RNA synthesis. J. Virol. **64:**1573–1583.
15. **Krieger, E., G. Koraimann, and G. Vriend.** 2002. Increasing the precision of comparative models with YASARA NOVA—a self-parameterizing force field. Proteins **47:**393–402.
16. **Lama, J., A. V. Paul, K. S. Harris, and E. Wimmer.** 1994. Properties of purified recombinant poliovirus protein 3aB as substrate for viral proteinases and as co-factor for RNA polymerase 3Dpol. J. Biol. Chem. **269:**66–70.
17. **Macias, M. J., S. Wiesner, and M. Sudol.** 2002. WW and SH3 domains, two different scaffolds to recognize proline-rich ligands. FEBS Lett. **513:**30–37.
18. **Molla, A., K. S. Harris, A. V. Paul, S. H. Shin, J. Mugavero, and E. Wimmer.** 1994. Stimulation of poliovirus proteinase 3Cpro-related proteolysis by the genome-linked protein VPg and its precursor 3AB. J. Biol. Chem. **269:**27015–27020.
19. **Neznanov, N., A. Kondratova, K. M. Chumakov, B. Angres, B. Zhumabayeva, V. I. Agol, and A. V. Gudkov.** 2001. Poliovirus protein 3A inhibits tumor necrosis factor (TNF)-induced apoptosis by eliminating the TNF receptor from the cell surface. J. Virol. **75:**10409–10420.
20. **Paul, A. V., X. Cao, K. S. Harris, J. Lama, and E. Wimmer.** 1994. Studies with poliovirus polymerase 3Dpol. Stimulation of poly(U) synthesis in vitro by purified poliovirus protein 3AB. J. Biol. Chem. **269:**29173–29181.
21. **Paul, A. V., J. H. van-Boom, D. Filippov, and E. Wimmer.** 1998. Protein-primed RNA synthesis by purified poliovirus RNA polymerase. Nature **393:**280–284.
22. **Porter, A. G.** 1993. Picornavirus nonstructural proteins: emerging roles in virus replication and inhibition of host cell functions. J. Virol. **67:**6917–6921.
23. **Reed, L. J., and H. Muench.** 1938. A simple method of estimating fifty per cent endpoints. Am. J. Hyg. **27:**493–497.
24. **Rust, R. C., L. Landmann, R. Gosert, B. L. Tang, W. Hong, H. P. Hauri, D. Egger, and K. Bienz.** 2001. Cellular COPII proteins are involved in production of the vesicles that form the poliovirus replication complex. J. Virol. **75:**9808–9818.
25. **Schlegel, A., T. H. Giddings, Jr., M. S. Ladinsky, and K. Kirkegaard.** 1996. Cellular origin and ultrastructure of membranes induced during poliovirus infection. J. Virol. **70:**6576–6588.
26. **Strauss, D. M., L. W. Glustrom, and D. S. Wuttke.** 2003. Towards an understanding of the poliovirus replication complex: the solution structure of the soluble domain of the poliovirus 3A protein. J. Mol. Biol. **330:**225–234.

27. **Suhy, D. A., T. H. Giddings, Jr., and K. Kirkegaard.** 2000. Remodeling the endoplasmic reticulum by poliovirus infection and by individual viral proteins: an autophagy-like origin for virus-induced vesicles. J. Virol. **74:**8953–8965.
28. **Toomre, D., P. Keller, J. White, J. C. Olivo, and K. Simons.** 1999. Dual-color visualization of *trans*-Golgi network to plasma membrane traffic along microtubules in living cells. J. Cell Sci. **112:**21–33.
29. **Towner, J. S., T. V. Ho, and B. L. Semler.** 1996. Determinants of membrane association for poliovirus protein 3AB. J. Biol. Chem. **271:**26810–26818.
30. **van Kuppeveld, F. J. M., J. M. D. Galama, J. Zoll, and W. J. G. Melchers.** 1995. Genetic analysis of a hydrophobic domain of coxsackie B3 virus protein 2B: a moderate degree of hydrophobicity is required for a *cis*-acting function in viral RNA synthesis. J. Virol. **69:**7782–7790.
31. **Vriend, G.** 1990. WHAT IF: a molecular modeling and drug design program. J. Mol. Graph. **8:**52–56.
32. **Williamson, M. P.** 1994. The structure and function of proline-rich regions in proteins. Biochem. J. **297:**249–260.
33. **Wimmer, E., C. U. Hellen, and X. Cao.** 1993. Genetics of poliovirus. Annu. Rev. Genet. **27:**353–436.
34. **Xiang, W., A. Cuconati, D. Hope, K. Kirkegaard, and E. Wimmer.** 1998. Complete protein linkage map of poliovirus P3 proteins: interaction of polymerase 3Dpol with VPg and with genetic variants of 3AB. J. Virol. **72:**6732–6741.
35. **Xiang, W., A. Cuconati, A. V. Paul, X. Cao, and E. Wimmer.** 1995. Molecular dissection of the multifunctional poliovirus RNA-binding protein 3AB. RNA **1:**892–904.